

Article

# Effect of In-Shoe Foot Orthosis Contours on Heel Pain Due to Calcaneal Spurs

Dwi Basuki Wibowo <sup>1,\*</sup>, Achmad Widodo <sup>1</sup>, Gunawan Dwi Haryadi <sup>1</sup>, Wahyu Caesarendra <sup>1,2</sup>   
and Rudiansyah Harahap <sup>3</sup>

<sup>1</sup> Mechanical Engineering Department, Diponegoro University, Jl. Prof. Soedharto, SH, Tembalang, Semarang 50275, Indonesia; awidodo2010@gmail.com (A.W.); gunawan\_dh@ft.undip.ac.id (G.D.H.); wahyu.caesarendra@ubd.edu.bn (W.C.)

<sup>2</sup> Faculty of Integrated Technologies, Universiti Brunei Darussalam, Jalan Tungku Link, BE1410, Brunei Darussalam

<sup>3</sup> Department of Orthopedic, RSUD Tugurejo Semarang, Semarang 50185, Indonesia; rudiansyahrsutugurejo@gmail.com

\* Correspondence: ir.dwibasuki.ms@gmail.com; Tel.: +62-812-298-9124

Received: 27 November 2018; Accepted: 25 January 2019; Published: 31 January 2019



**Featured Application:** The proposed method for easily obtaining contoured insoles from the variation of the insole foot area together with the pain pressure threshold could potentially be applied to orthotic shoe designers for reducing pain in calcaneal spur patients.

**Abstract:** The objective of this study is to investigate the effect of contouring the shoe insole on calcaneal pressure and heel pain in calcaneal spur patients. Calcaneal pressure was measured using three force sensors from 13 patients including three males and 10 females. These patients have plantar heel pain due to calcaneal spurs, and we examined five customized contour insole foot areas (0–100%). Sensors were attached at the central heel (CH), lateral heel (LH) and medial heel (MH) of the foot. The pain was measured using an algometer and evaluated by the pain minimum compressive pressure (PMCP). In this study, it was observed that the calcaneal pressure decreased with increasing insole foot area. In addition, increasing the insole foot area from 25% to 50% can reduce the calcaneal pressure approximately 17.4% at the LH and 30.9% at the MH, which are smaller than the PMCP, while at the MH, pressure reduced 6.9%, which is greater than the PMCP. Therefore, to reduce pain, one can use 50% insole foot area, even though at MH it is still 19.3% greater than the PMCP. Excellent pain relief was observed when using 100% insole foot area, as the pressures in those three areas are lower than the PMCPs, but it is not recommended because it requires large production costs.

**Keywords:** calcaneal spur; pain minimum compressive pressure; contour of shoe insole; insole foot area

## 1. Introduction

Plantar heel pain is one of the most common musculoskeletal conditions affecting the foot in adults, with a highest incidence at the age of 40 to 60 years [1,2]. There are many causes of pain in the plantar heel area, and one of them is due to a calcaneal/heel spur [3].

A calcaneal spur is a condition where a calcium deposit grows between the heel and arch of the foot [4]. Generally, this does not affect a person's daily life, but repetitive stress from activities may result in the spur breaking into sharp pieces and pressing the nerves of the plantar fascia [5–7]. This condition causes plantar fasciitis, in which patients experience pain and tenderness at the heel [8,9]. People who are obese, individuals with either flat feet or high arches, and individuals who engage in prolonged standing or walking are very vulnerable to this disease [6].

Heel pain treatment (including pain caused by a calcaneal spur) is listed in the document of the Clinical Practice Guideline (CPG) developed by the heel pain committee of the American College of Foot and Ankle Surgeons (ACFAS), which recommends quick procedures in assessment and management of heel pain [10]. The authors classify treatments into three phases for heel pain treatments, and the use of orthotic shoes is recommended in phase II.

Orthotic shoes for calcaneal spur patients are specially designed to reduce pain when used for walking activity by modifying pressure in the heel region [11,12]. Pressure reduction using orthotic shoes requires knowledge of the location and dimensions of the spur, and typically the minimum pressure that causes pain in the patient's heel area. A large-dimension spur ( $\geq 6$  mm) causes high pain level compared to a small spur (1–2 mm) [13]. Determining the area in the heel where the spur growth is plays a major role in knowing the level of the pain. The research on pressure pain threshold (PPT) in patients experiencing plantar heel pain syndrome using a pressure algometer was presented by Saban et al. [14]. To measure PPT, the heel was divided into five regions. The results indicated that PPT levels at posterior/medial, anterior/medial and central regions were significantly lower than at anterior/lateral and posterior/lateral regions.

Various types of shoe soles have been studied to reduce pain in the heel area. Shoes with thick soles and extra cushioning can reduce pain while standing and walking [15,16]. High-heel shoes can shift pressure away from the heel to the mid-foot and fore-foot [17]. Contoured insoles are better than flat insoles in reducing local peak pressures [18–20]. A number of methods have been carried out to estimate the contact pressures or pressure distribution patterns in both feet for each subject during standing and/or walking activity. The methods applied the finite element method (FEM) [15], used a pressure sensor, that is, the Force Sensing Resistor (FSR) [16,17], were based on a weighting scale method [18], used a flexible F-Scan<sup>®</sup> insole sensing system [19], or used capacitance sensor/transducers (the PEDAR<sup>®</sup> pressure measurement system) [20].

Commonly, to obtain a contour-customized in-shoe foot orthotics is done by taking a plaster cast of the patient's foot plantar surface (the negative cast) and then moulding this negative cast on a plaster casting board to obtain the positive cast [21]. Tsung et al. [18] made the positive cast with full-weight-bearing and semi-weight-bearing by directly printing the plantar foot on the casting board placed on top of the electronic balance. Another method to obtain the patient's foot plantar surface is to use 3D scanning, which is the latest technology that has been widely used by many researchers [22,23]. This study aims to determine the effect of contouring of an in-shoe foot orthosis on heel pressure while standing, and its relationship to the pain in the heel area.

## 2. Materials and Methods

Thirteen patients (3 male and 10 female) at the local public hospital Tugurejo Semarang with plantar heel pain due to a calcaneal spur from June 2017 to August 2018 were involved in the experimental work of the study. The ethical clearance has been approved and issued by the Ethics Committee of the Tugurejo Hospital. All subjects have also signed and provided their written informed consent before participating in this study. The diagnosis of plantar heel pain of the patients was based on pain upon palpation. The mean age of the subjects was  $56.5 \pm 9.9$  years (range between 38–73 years), mean height was  $155.6 \pm 7.6$  cm (range from 144 to 172 cm) and mean weight was  $63.3 \pm 9.4$  kg (range between 50–84.6 kg). The location and dimension of each patient's spur were obtained from lateral X-rays [17]. The length of the spur is classified into 3 types: small (1–2 mm), medium (3–5 mm) and large ( $\geq 6$  mm) [13]. There were 7 patients with a calcaneal spur on both feet, but in this study, only the longest spur was evaluated because there is a significant correlation between the length of spur and the pain minimum compressive pressure (PMCP) [17].

In order to obtain an exact location and dimension of the spur in the plantar view as shown in Figure 1 up, each patient was requested to do a two-dimensional footprint using a digital footprint scanner (LSR 2D Laser Foot Scanner, Vismach Technology Ltd., China). This scanner is equipped with software to measure foot length (FL) and foot width (FW) to determine the shoe size and heel width

(HW) of each patient [24]. The spur is assumed to be located in the heel center line, which is a line drawn from the center of the heel (CH) to the tip of the second toe [25].

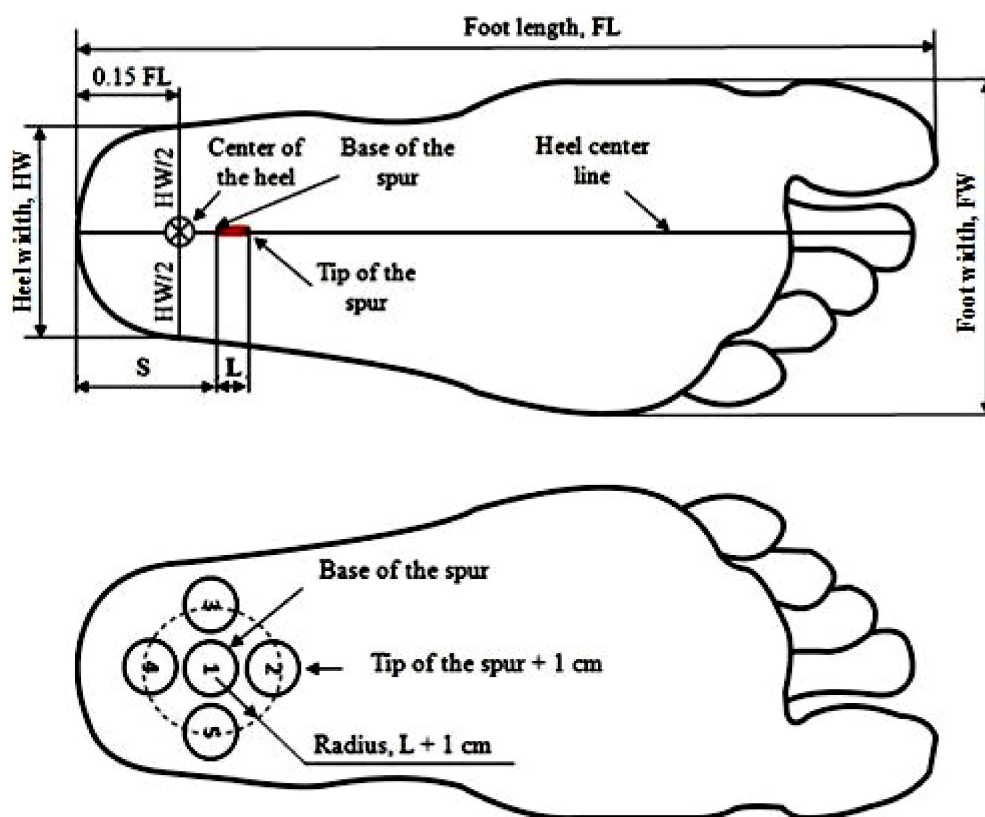


**Figure 1.** (up) Location and dimension of the spur in the plantar view; (down) Five locations of the pressure pain threshold (PPT) around spur growth.

The pain in the heel area was measured using an FDIX 25 algometer (Wagner Instruments, Greenwich CT, USA), which consists of a flat rubber tip probe 1.0 cm in diameter [26]. This instrument can display the compression force in either Newtons or kilograms and also can measure the pressure which is calculated from the force divided by the probe area. The region of the pain pressure threshold (PPT) was determined around the spur growth which is divided into five points: point 1 at the base of the spur, and the next compressive test points at the anterior site (point 2), the lateral site (point 3), the posterior site (point 4), and the medial site (point 5), made circular with radius of spur length,  $L$  plus 1 cm as presented in Figure 1 down. The addition of 1 cm is needed to compensate for the diameter of the algometer probe. The calculation method of PPT region in this paper is similar to the study conducted by Saban et al., but the exact location of pain suppression was not specified and the patients recruited were not specifically recruited due to the calcaneal spur [14].

To measure PPT, the patient was requested to lay supine in a relaxed position and press the algometer probe at point 1 as shown in Figure 1 down.  $S$  is the distance from the tip of the heel to the base of the spur and  $L$  is the length of the spur. We increased the pressure gradually until the patient complained of pain. We recorded the pressure value and applied a similar procedure to others points. From the recorded data, the PMCP and the point location in each patient can be monitored [17].

### 2.1. Determining the Contour of the Shoe Insole

In this study, the negative cast of the custom insole foot contour is made from a 3D foot scanner (ScanPod 3D, Vismach Technology Ltd., Hongkong, China). The accuracy of this scanner is  $\pm 1.0 \text{ mm}$  and the output is in the standard language (dxf/stl/wrl/obj/ply/asc). These formats are associated with any 3D software, for example, AutoCAD. The output can be in the form of the 3D plantar the of

foot in difference of colors as presented in Figure 2a, where the red color indicates where the foot has the largest convex (largest z-coordinates), the 3D foam negative impression to make a negative cast of the foot as shown in Figure 2b, and the 3D positive model of the footprint in the form of a foam impression as shown in Figure 2c [27].

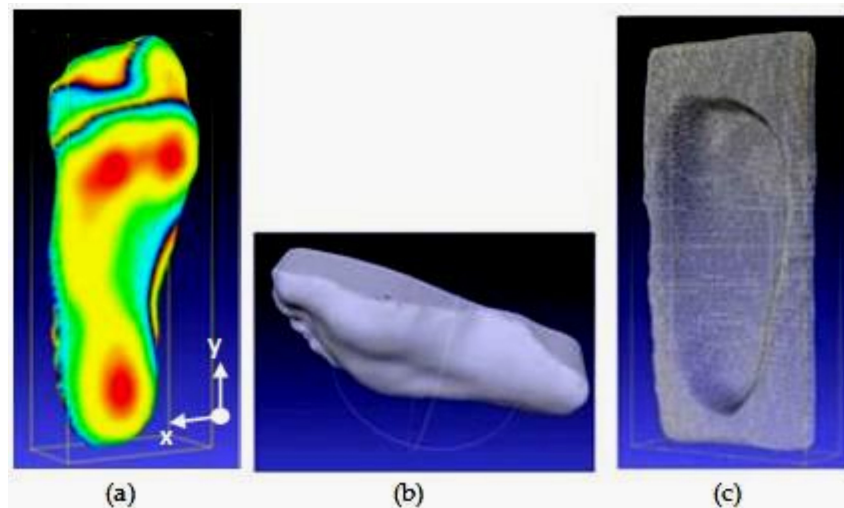


**Figure 2.** Example outputs of 3D scanning: (a) footprint depth in difference of colors; (b) 3D foam negative impression; (c) footprint 3D positive model.

This technique has been used previously by Telfer et al. [22] and Stankovic et al. [23]. The difference between the technique proposed in this paper and the above-mentioned published papers is in the variation of the shape of the foot that was evaluated. In this study, the shoe insole foot contours are distinguished by the insole foot area, where the largest area is equal to the contour of the unloaded foot (100% A) and the smallest is the same as the flat insole (0% A). This is based on the fact that the sole of the foot will follow the contour of the shoe insole as long as it does not exceed the contour of the unloaded foot. There were 5 variations of shoe insole foot area, that is, (1) 100% A, (2) 75% A, (3) 50% A, (4) 25% A, and (5) 0% A. One hundred percent and zero percent areas express the contour and projection areas of the 3D scanning result of the foot evaluated using Rhinoceros software, respectively. The other shoe insole area is calculated as follows:

$$n\% A = n\% \times \Delta A + 0\% A, \quad (1)$$

where n are 75, 50 and 25 and  $\Delta A = 100\% A - 0\% A$ .

Varying the area of shoe insole means changing the z-coordinates at 100% A until it reaches z-coordinates at 75% A to 25% A. The procedure for determining variations of the shoe insole area is presented in detail in Figure 3a. The following steps are conducted in the experimental work:

Scan the foot in 3D format and import this 3D scanned image file into AutoCAD.

- (1) Evaluate the area 100% A and 0% A using Rhinoceros software.
- (2) Generate the xyz-coordinates of 100%\_A by using Microsoft Excel which integrated with AutoCAD software as presented in Figure 3b.
- (3) Adjust the z-coordinates of 100% A to 75% A; initially specify a reduced percentage of 5% (reduced percentage z-coordinates of 100% A and 0% A are 0% and 100%, respectively) and display the coordinates in AutoCAD to evaluate its area using Rhinoceros software.
- (4) If the area is still much greater than 5 mm<sup>2</sup> [28] compared with Equation (1), repeat the procedure four times by increasing the percentage of 5% reduction.
- (5) If the difference of area approaches 5 mm<sup>2</sup>, increase the percentage reduction to 1–2%.

A similar procedure (step 4 to 6) is conducted to obtain shoe insole area of 50% A and 25% A by initially determining that the deduction percentage is slightly greater than the deduction percentage of 75% and 50%, respectively. The z-coordinates for every n% A can then be calculated using Equation (2), where z, z<sub>max</sub> and z<sub>min</sub> express the z-coordinates at 100% A (z<sub>100%\_A</sub>) and the largest and smallest z-coordinates at 100% A, respectively.

$$z_{n\%A} = z - \left( \frac{2z - (z_{\max} + z_{\min})}{2} \right) \times \% \text{ deduction} \tag{2}$$

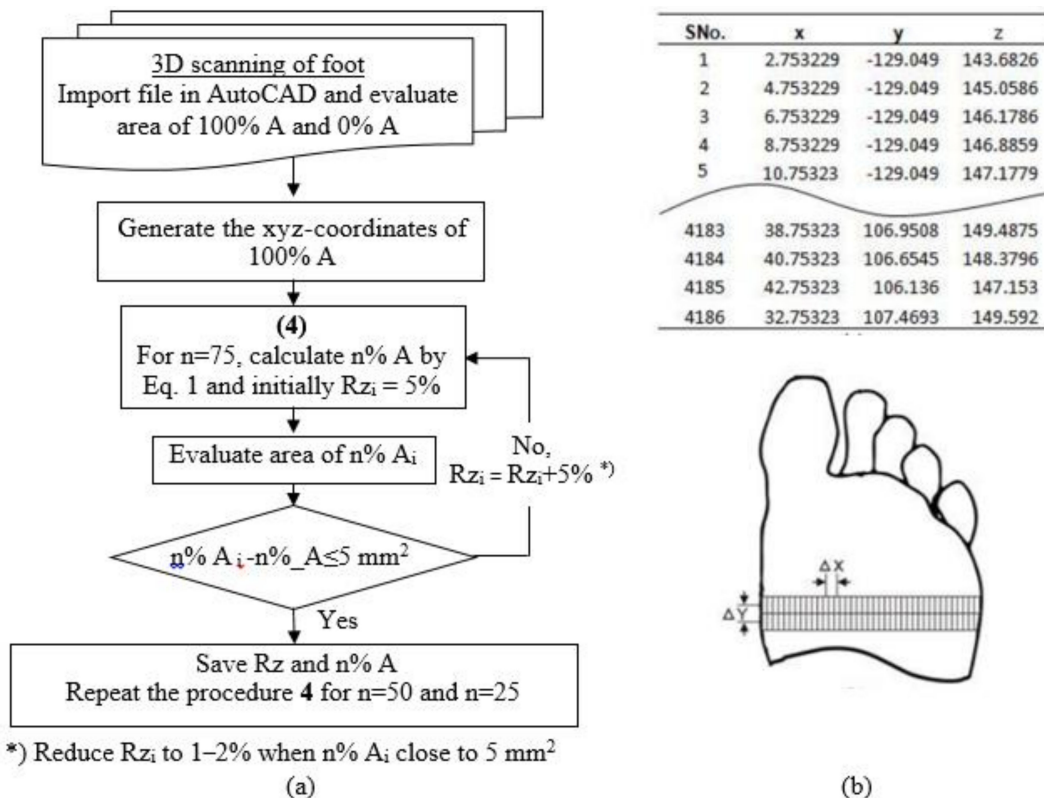


**Figure 3.** (a) Flowchart evaluation of n% insole foot area; (b) Table of 3D coordinates (x, y, and z axis) generated from AutoCAD with the visualization of the increment of x- and y-axis.

### 2.2. Measuring Pressure in Heel Area

To measure the burden of its own weight, we used three force sensing resistors (FSR 402, Interlink Electronics) which are attached to the calcaneal area of the feet with double tape. Determination of the location of each sensor was performed using an unloaded foot scan around the area that was estimated to receive a large burden when standing, as shown in Figure 2a. For this purpose, sensor 2 is placed at CH (0.15 FL) [29] and sensors 1 and 3 are placed arbitrarily at the lateral heel (LH) and medial heel (MH), in line above sensor 2, under the boundary between the heel and mid foot area (0.31 FL) [30], as shown in Figure 4.

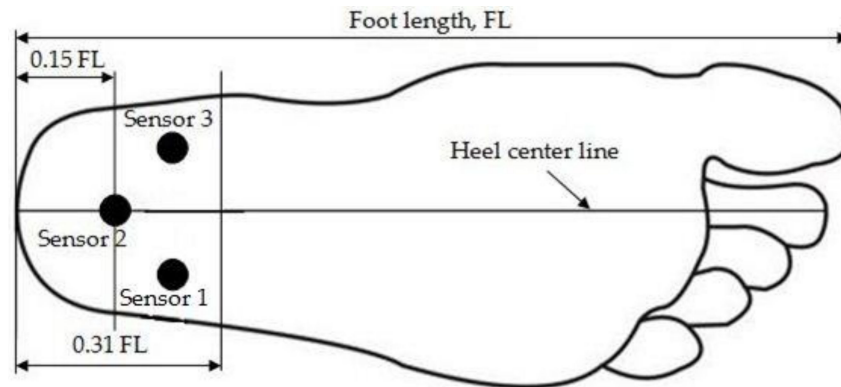


**Figure 4.** Illustration of the Force Sensing Resistor (FSR) sensor locations.

The FSR is a polymer thick-film device which exhibits a decrease in resistance with an increase in the force applied to the active surface. Its force sensitivity is optimized for use in human touch control of electronic devices. FSRs are not a load cell or strain gauge, though they have similar properties. The FSR 402 has active area of 0.5" (12.7 mm) diameter, the nominal thickness of 0.018" (0.46 mm), force sensitivity range of 100 g to 10 kg, and pressure sensitivity range of 1.5 to 150 psi. The relationship between the load  $L$  (grams) and the voltage  $V$  (volts) can be expressed by polynomial regression, as presented in Equation (3). Each sensor is connected to one resistor. The output voltage of the FSR sensor is read by the Arduino MEGA 2560 microcontroller using 10 pin analog input bits [31]. Then, the voltage is sent to DAQ software LabVIEW via serial USB to be converted into load using Equation (3).

$$L = 927.7 V^3 - 1643.9 V^2 + 1083.5 V - 31.02 \quad (3)$$

Each patient was requested to stand upright using the appropriate test shoe size for each shoe insole area. The outsole material is made of Microcell Puff EVA foam and the insole made of Poron cushioning [32]. Initially, each patient is requested to wear the shoe with 0% A, and three pressure datapoints from CH, MH and LH areas are recorded. A similar procedure is carried out for the 25% A, 50% A and 100% A, and the results are compared to the value of PMCP which is measured using an algometer. The patient will feel pain if the pressure in the heel region is greater than the PMCP.

### 3. Results

Among the 13 patients, seven patients had symptomatic heel spurs on two feet. Since the longest spur was used in this study, a total of 20 feet were evaluated. The length of spur ( $L$ ) ranged between 1.5 and 7 mm, as presented in detail in Table 1. According to Table 1, three classifications are determined: (1) there are two patients with small length of spur, with average  $L$  of  $1.75 \pm 0.35$  mm; (2) there are seven patients with medium length of spur, with average  $L$  of  $3.93 \pm 0.73$  mm; and (3) there are four patients with large length of spur, with average  $L$  of  $6.50 \pm 0.58$  mm. Based on data of FL and FW, we can obtain the shoe size of each patient [33]; one patient has shoe size 37; four patients have shoe size 38; one patient has shoe size 39; four patients have shoe size 40; two patients have shoe size 42; and one patient has shoe size 43. Thus, we summarize a total of six shoe sizes of 37–40 and 42–43. Each size is not made in the shoe form, but in the form of a foam impression (Figure 2c), and for variation in the shoe insole area of 0% A to 100% A, a total of 30 foam impressions were made. The distance measurements of the center of the heel (used for pressure measurement of sensor 2, Figure 1 up) and the base of the spur (used for PPT measurement of point 1, Figure 1 down) are not coincident. The distance from the center of the heel (CH) ranged between 35.1–41.4 mm, and the distance from the base of spur ( $S$ ) ranged between 30–41 mm, where there were seven patients with the base of spur location on the right CH and six other patients at the left CH (the farthest distance of  $S$  and CH is 7 mm, and the closest is 0.4 mm).

**Table 1.** A detailed description of each subject.

Subject Number	1	2	3	4	5	6	7	8	9	10	11	12	13
Height, cm	155	157	151	153	153	172	150	156	146	159	164	163	144
Weight, kg	57.2	60	50	52	70	63.8	59	68.6	55.3	84.6	62.7	72	67.6
FL, mm	249	266	237	240	252	276	237	251	240	240	270	273	234
FW, mm	98	118	106	91	100	108	96	102	94	100	100	99	90
Shoe size	40	42	38	38	40	43	38	40	38	39	40	42	37
L, mm	4.5	3.0	1.5	4.0	5.0	3.0	4.0	7.0	6.0	7.0	2.0	4.0	6.0
CH, mm	37.4	39.9	35.6	36.0	37.8	41.4	35.6	37.7	36.0	36.0	40.5	41.0	35.1
S, mm	38.0	34.0	36.0	38.0	39.0	41.0	35.0	39.0	30.0	38.0	34.0	34.0	36.0
(CH-S), mm	-0.6	5.9	-0.5	-2.0	-1.2	0.4	0.5	-1.4	6.0	-2.0	6.5	7.0	-0.9

The information on the results of PMCP measurements at each heel site is very important to know which sites have the smallest PMCP value. Table 2 shows the pressure pain sensitivity in patients with plantar heel pain due to a calcaneal spur at each heel site, where the PMCP ranged between 1.24–3.3 kg/cm<sup>2</sup> and averaged 2.09 ± 0.63 kg/cm<sup>2</sup>. The result shows that the smallest PMCP occurs at the anterior site, and the PMCP at the medial site was significantly lower than at the lateral site.

**Table 2.** The pain minimum compressive pressure (PMCP) values at each heel site.

Heel Site	Number of Feet	PMCP (kg/cm <sup>2</sup> ) Mean ± SD (Range)	PMCP Related to the Length of Spur Types (kg/cm <sup>2</sup> ) Mean ± SD (Number of Feet)		
			Small	Medium	Large
			1	1	1.32
2	5	1.63 ± 0.25 (1.24–1.87)	-	1.24 (1)	1.73 ± 0.13 (4)
3	2	3.13 ± 0.25 (2.95–3.3)	2.95 (1)	3.3 (1)	-
4	2	2.38 ± 0.37 (2.11–2.64)	-	2.38 ± 0.37 (2)	-
5	3	2.25 ± 0.41 (1.92–2.71)	-	2.25 ± 0.41 (3)	-

The procedure to obtain n% insole foot area (Figure 3) produces the values of percentage deductions that can be applied to all of the shoe insoles (Table 3). The contour results of the foot of the shoe insole area of 0% A to 100% A from one of the study subjects are shown in Figure 5.

**Table 3.** The deduction percentage and area of shoe insole result of modification of z-coordinate and calculation using Equation (1) from one of the study subjects.

% Shoe Insole Area	% Deduction	Shoe Insole Area (mm <sup>2</sup> )	
		From Modification of z-Coordinates	From Equation (1)
100	0	17,972	17,972
75	16.5	17,063	17,071
50	34.5	16,169	16,170
25	56	15,266	15,269
0	100	14,368	14,368

According to the body weight (BW), there was a relationship between BW and the pressure in the calcaneal region. As the BW increases, the pressure at MH, LH and CH will increase as well [6]. There was a significant increase in pressure for the MH area, except at 100% A, with an average correlation coefficient of 0.74. At LH, a significant increase in pressure is seen at 0–50% A with an average correlation coefficient of 0.85. Furthermore, at CH, a significant increase in pressure is seen at 0–25% A with an average correlation coefficient of 0.85. To find the effect of area of shoe insole on the pressure of each pressure sensor in detail, it is easier to use a comparison of the pressure of each sensor to the BW or the total pressure of all sensors. Table 4 shows the distribution of pressure on the calcaneal region of one foot (assumed to be the same between left and right feet), expressed as

a proportion of BW and the percentage of each sensor to the total pressure of all of the sensors. In comparison to the BW, it is seen that the percentage area of the shoe insole is increased. However, the peak pressure is decreased for the MH, LH and CH. The significant decreases are seen at the MH of 75% to 100% A and at the LH of 50% to 75% A and 75% to 100% A, respectively. In comparison to the total pressure of all sensors seen, there is a significant increase at the MH of 50% to 75%. In contrast, the pressure at the LH shows a significant decrease at the same percentage areas of shoe insole.

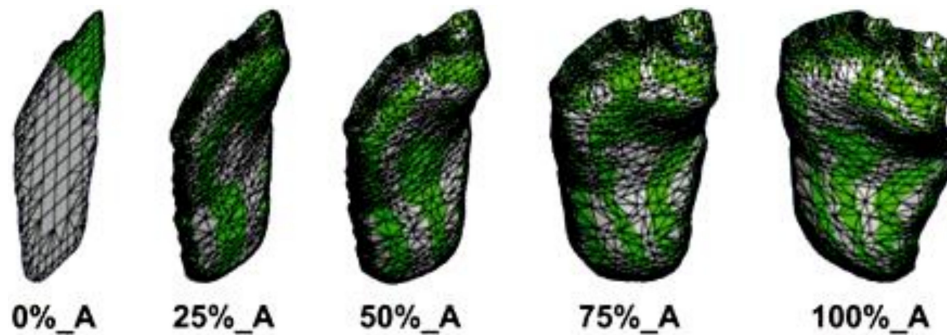


Figure 5. Example of negative casts of the foot from one subject.

Table 4. Comparison of load of each sensor to the BW and all sensors (%).

Percentage Area of Shoe Insole	0%	25%	50%	75%	100%
Calcaneal region	Comparison to the BW (mean ± SD)				
MH	10.14 ± 1.46	8.93 ± 1.16	8.26 ± 1.65	7.01 ± 1.09	3.64 ± 0.60
LH	7.46 ± 1.28	6.70 ± 1.06	5.53 ± 0.91	2.23 ± 0.52	0.93 ± 0.16
CH	1.44 ± 0.20	1.05 ± 0.21	0.73 ± 0.09	0.59 ± 0.09	0.24 ± 0.06
Calcaneal region	Comparison to all sensors (mean ± SD)				
MH	53.31 ± 0.82	53.60 ± 1.55	56.69 ± 1.26	71.49 ± 2.36	75.47 ± 3.04
LH	39.11 ± 1.01	40.11 ± 1.04	38.20 ± 0.78	22.44 ± 2.55	19.44 ± 2.41
CH	7.58 ± 0.18	6.29 ± 0.51	5.11 ± 0.48	6.07 ± 0.20	5.09 ± 1.03

The distribution of loading at the MH, LH and CH for the five percentage areas of shoe insole is shown in Figure 6. The pressure applied at the CH is lower than the PMCP for all percentage areas of the shoe insole, while the pressure at the LH is lower than the PMCP with increasing percentage area of shoe insole from 25%. The magnitude of pressure is significantly greater than PMCP at the MH of 0% to 50% A (that is, 34.07%, 25.09% and 19.30% of PMCP, respectively). In relation to the length of spur, the pressures applied at the MH, LH and CH for five percentage areas of shoe insole are shown in Table 5 and Figure 7. As percentage area of shoe insole increased, the pressure in the calcaneal region decreased for all lengths of the spur. For the small and medium lengths of spur, the pressure at MH is greater than PMCP at percentage area of shoe insole 0–50%, while for the large length of spur, the pressure at MH is greater than PMCP at percentage area of shoe insole 0–75%. At LH, the pressure is slightly higher than PMCP at small length of spur only in the 0% A, while at the medium length of spur, the pressure is lower than PMCP for all percentage areas of shoe insole. For large lengths of spur, the pressure at the LH is greater than the PMCP in the percentage area of shoe insole 0–50%. The significant lowered pressure is seen at the CH for all lengths of spur and percentage areas of the shoe insole, compared to the PMCP.

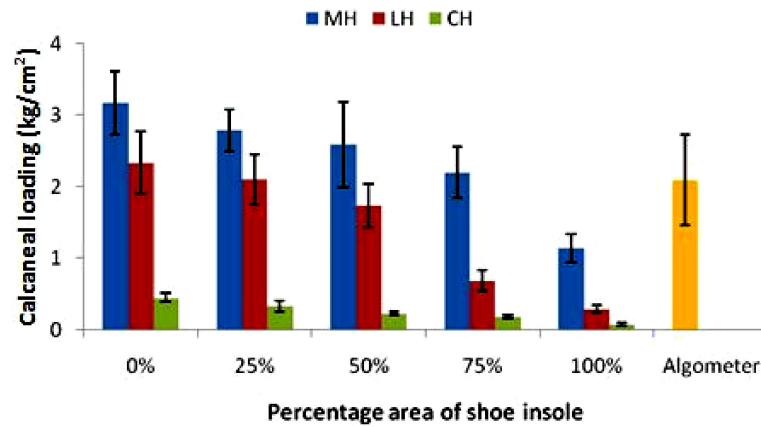


Figure 6. Calcaneal loading during standing for the five percentage areas of shoe insole, compared to the PMCP measured using the algometer (mean ± SD).

Table 5. The distribution of pressure at the MH, LH and CH for each length of spur.

Spur Length	PMCP (kg/cm <sup>2</sup> )	Calcaneal Region	Calcaneal Loading for Each Percentage Area of Shoe Insole (kg/cm <sup>2</sup> )				
			0%	25%	50%	75%	100%
Small	2.14 ± 1.15	MH	3.00 ± 0.34	2.67 ± 0.22	2.37 ± 0.45	2.06 ± 0.27	1.02 ± 0.10
		LH	2.17 ± 0.34	1.96 ± 0.27	1.61 ± 0.24	0.69 ± 0.15	0.27 ± 0.04
		CH	0.43 ± 0.05	0.30 ± 0.06	0.22 ± 0.02	0.17 ± 0.02	0.05 ± 0.00
Medium	2.29 ± 0.66	MH	3.11 ± 0.33	2.75 ± 0.21	2.52 ± 0.43	2.15 ± 0.26	1.18 ± 0.22
		LH	2.28 ± 0.32	2.06 ± 0.26	1.70 ± 0.23	0.68 ± 0.11	0.29 ± 0.04
		CH	0.44 ± 0.04	0.32 ± 0.06	0.23 ± 0.02	0.18 ± 0.02	0.08 ± 0.01
Large	1.73 ± 0.13	MH	3.35 ± 0.69	2.91 ± 0.45	2.84 ± 0.91	2.34 ± 0.56	1.13 ± 0.18
		LH	2.52 ± 0.68	2.24 ± 0.54	1.86 ± 0.48	0.71 ± 0.22	0.31 ± 0.08
		CH	0.47 ± 0.09	0.36 ± 0.12	0.24 ± 0.03	0.20 ± 0.04	0.09 ± 0.03

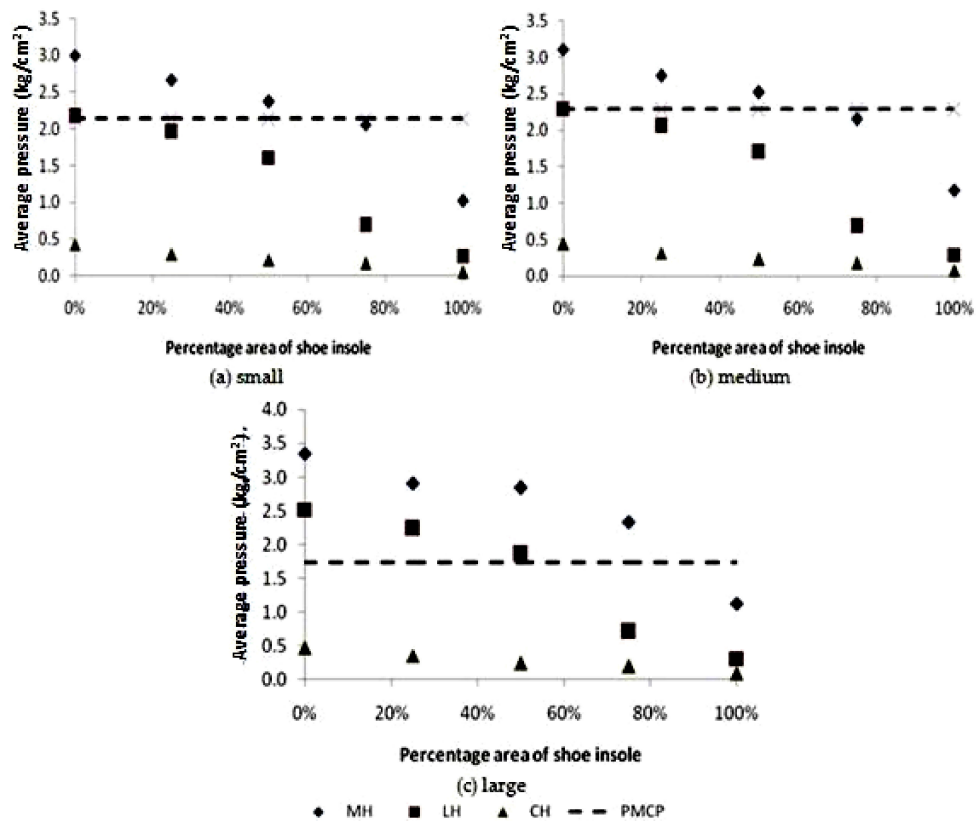


Figure 7. The pressure at the MH, LH and CH for the five percentage areas of shoe insole and each length of spur, as presented in Table 5.

#### 4. Discussion

The determination of PPT location as a function of base and length of spur (Figure 1 down) is necessary for obtaining an accurate PMCP value and the point location in each patient. The results of PPT from 13 patients, as shown in Table 2, showed that the PMCP occurs mostly at the anterior site (that is, 38.5%). This result is similar to previously published work reported by Goff et al. [6] and Wibowo et al. [17]. These PPT results are also in accordance with the study of Saban et al. [14], which indicated that the average PMCP at the medial site was significantly lower than the one at the lateral site (that is, 2.25 and 3.13 kg/cm<sup>2</sup>, respectively).

The research for obtaining the contour of the sole by varying the contact area of the foot using 3D scanners is a novelty. By using a 3D foot scanner [22,23,27], it is easier to obtain a form of a shoe insole mold (foot impression cast) than previously, which involved placing the sole of a foot on a gypsum mold for any different bearing conditions [18,19]. The procedure that is described in Figure 3a can be applied to determine any foot impression cast shape of the shoe insole area. For example, it is desirable to get a foot impression cast shape shoe insole area of 70%; the initial value of the percentage of z deduction can be set to 10% (Table 3). The generating xyz-coordinates obtained from Equation (2) can be made into a 3D negative cast model from wood (Figure 5) by using Computer Numerical Control (CNC) milling.

Table 4 is used to check the validity of load measurements and the position of the foot during standing. In comparison to the BW, at 0% A, it shows that the subjects' feet support a total load of 19.04% of BW in the calcaneal region. This result is similar to the previous study of 19.32% BW presented in Ref. [34]. In comparison to the total pressure of all sensors, the pressure at MH is larger than at LH for all insole foot areas, which indicates that most of the patients' heels tend to pronation while standing [35,36]. The pronation tendency occurs very clearly in 75% A and 100% A, and are possibly caused by the sensor mounted at the LH shifting to the heel center line for holding pain, seen from the significant decrease in load to only 22.44% and 19.44%, respectively, compared to MH.

This study proved that contoured insoles are better than flat insoles in reducing local peak pressures [18–20], but in relation to pressure relieving pain, are only 100% A at MH and 50–100% A at LH, which are lower pressures than the PMCPs. The pressures at CH are all lower than PMCP for the all insole foot areas (Figure 6). These results are corresponding to the research conducted by Chia et al. [16] and Bonanno et al. [37], and prove that the contoured insole increases foot area contact and reduces pain pressure in the calcaneal region. To find the percentage of insole foot areas suitable for each patient without causing pain in detail, we can examine the evaluation of pressure in the calcaneal region associated with the types of spur length (Table 5). For large spur lengths there are four patients requiring a 100% A; for the medium spur lengths there is one patient requiring 50% A, five patients requiring 75% A, and one patient requiring 100% A; while for small spur lengths there are two patients requiring 50% A and 100% A, respectively.

The average difference between the location of the base of the spur (S) and the location of the center of the heel (CH) was 1.37 mm (Table 1). Therefore, the position of the CH as the basis for the measurement of pressure using the FSR sensor was relatively accurate, since the area of the sensor was still able to compress the base of the spur.

#### 5. Conclusions

The main criterion for the use of a contoured orthotic shoe insole for heel pain sufferers due to a calcaneal spur depends on how well it can reduce pain when used for standing. Therefore, the information on how the shape of the contour of the foot changes with weight bearing, which results in the smallest pain at the heel area, is essential in shoe design. This quantitative study shows that it is easy to obtain a variety of shoe insole foot contours by varying the contact area of the shoe insole, compared to directly printing the plantar foot on the casting board for any weight bearing condition. The use of larger insole areas could reduce local peak pressure. Contoured insoles were significantly better than flat insoles.

To reduce pain in patients with a calcaneal spur while standing, we can use 50–100% insole foot area. The average pressures at CH and LH for a 50% insole foot area are 0.23 kg/cm<sup>2</sup> and 1.73 kg/cm<sup>2</sup>, respectively, which are significantly lower than the average PMCPs (89.0% and 17.1%, respectively), while the average pressures at 75% insole foot area are 0.19 kg/cm<sup>2</sup> and 0.69 kg/cm<sup>2</sup>, respectively, which are also significantly lower than the average PMCPs (91.1% and 67.0%, respectively). On the other hand, the average pressures at MH for a 50% and 75% insole foot area are 2.59 kg/cm<sup>2</sup> and 2.20 kg/cm<sup>2</sup>, respectively, which are still greater than the average PMCPs (19.3% and 4.7%, respectively). One hundred percent insole foot area can also be used, but is not recommended—even though the average pressure in all regions and the percentage of insole foot area are smaller than the average PMCP—because it requires large production costs.

**Author Contributions:** Conceptualization, D.B.W.; methodology, D.B.W.; software, D.B.W. and W.C.; validation, A.W. and G.D.H.; formal analysis, D.B.W. and A.W.; investigation, G.D.H.; resources, G.D.H. and R.H.; data curation, W.C. and R.H.; writing—original draft preparation, D.B.W.; writing—review and editing, A.W. and W.C.; visualization, D.B.W., A.W. and W.C.; supervision, R.H.; project administration, G.D.H.; funding acquisition, D.B.W. and G.D.H.

**Acknowledgments:** This work was supported by the Superior Applied Research in higher education Directorate of Research and Community Service, Directorate General of Research and Development Strengthening, Indonesian Ministry of Research, Technology and Higher Education. Contract No: 101-155/UN7.P4.3/PP/2018.

**Conflicts of Interest:** The authors declare that there are no known conflicts of interest related to this project that could have influenced this manuscript.

## References

- Buchbinder, R. Clinical practice: Plantar fasciitis. *N. Engl. J. Med.* **2004**, *350*, 2159–2166. [CrossRef] [PubMed]
- McCarthy, D.J.; Gorecki, G.E. The anatomical basis of inferior calcaneal lesions: A cryomicrotomy study. *J. Am. Podiatry Assoc.* **1979**, *69*, 527–536. [CrossRef] [PubMed]
- Bartold, S.J. The Plantar Fascia as a Source of Pain – Biomechanics, Presentation and Treatment. *J. Bodyw. Mov. Ther.* **2004**, *8*, 214–226. [CrossRef]
- Barrett, S.L.; O'Malley, R. Plantar Fasciitis and Other Causes of Heel Pain. *Am. Fam. Physician* **1999**, *59*, 2200–2206. [PubMed]
- Smith, S.; Tinley, P.; Gilheany, M.; Grills, B. The inferior calcaneal spur-anatomical and histological considerations. *Foot* **2007**, *17*, 25–31. [CrossRef]
- Goff, J.D.; Crawford, R. Diagnosis and treatment of plantar fasciitis. *Am. Fam.* **2011**, *84*, 676–682.
- Zhou, B.; Zhou, Y.; Tao, X.; Yuan, C.; Tang, K. Classification of calcaneal spurs and their relationship with plantar fasciitis. *J. Foot Ankle Surg.* **2015**, *54*, 594–600. [CrossRef] [PubMed]
- Roberts, S. Scott's Book on Plantar Fasciitis, Heel Spurs, and Heel Pain. Available online: [http://heelspurs.com/\\_intro.html](http://heelspurs.com/_intro.html).
- Hyland, M.R.; Gaffney, A.; Cohen, L.; Lichtman, S.W. Randomized control trial of calcaneal taping, sham taping, and plantar fascia stretching for short-term management of plantar heel pain. *J. Orthop. Sports Phys. Ther.* **2006**, *36*, 364–371. [CrossRef]
- Thomas, J.L.; Christensen, J.C.; Kravitz, S.R.; Mendicino, R.W.; Schubert, J.M.; Vanore, J.V.; Weil, L.S., Sr.; Zlotoff, H.J.; Bouché, R.; Baker, J. The Diagnosis and Treatment of Heel Pain: A Clinical Practice Guideline—Revision 2010. *J. Foot Ankle Surg.* **2010**, *49*, S1–S19. [CrossRef]
- Kogler, G.; Solomonidis, S.E.; Paul, P.J. Biomechanics of longitudinal arch support mechanics in foot orthoses and their effect on plantar aponeurosis strain. *Clin. Biomech.* **1998**, *11*, 243–252. [CrossRef]
- Kogler, G.; Veer, F.; Solomonidis, S.E.; Paul, P.J. The influence of medial and lateral placement of orthotic wedges on loading of the plantar aponeurosis. *J. Bone Jt. Surg. Am.* **1999**, *81*, 1403–1413. [CrossRef]
- Ozdemir, H.; Soyuncu, Y.; Ozgorgen, M.; Dabak, K. Effects of changes in heel fat pad thickness and elasticity on heel pain. *J. Am. Podiatr. Med. Assoc.* **2004**, *94*, 47–52. [CrossRef] [PubMed]
- Saban, B.; Masharawi, Y. Pain threshold tests in patients with heel pain syndrome. *Foot Ankle Int.* **2016**, *37*, 730–736. [CrossRef] [PubMed]
- Cheung, J.; Zhang, M. A 3-dimensional finite element model of the human foot and ankle insole design. *Arch. Phys. Med. Rehabil.* **2005**, *86*, 353–358. [CrossRef]

16. Chia, J.K.; Suresh, S.; Kuah, A.; Ong, J.L.; Phua, J.M.; Seah, A.L. Comparative trial of the foot pressure patterns between corrective orthotics, formthotics, bone spur and flat insoles in patients with chronic plantar fasciitis. *Ann. Acad. Med. Sing.* **2009**, *38*, 869–875.
17. Wibowo, D.B.; Harahap, R.; Widodo, A.; Haryadi, G.D.; Ariyanto, M. The effectiveness of raising the heel height of shoes to reduce heel pain in patients with calcaneal spurs. *J. Phys. Ther. Sci.* **2017**, *29*, 2068–2074. [[CrossRef](#)] [[PubMed](#)]
18. Tsung, B.Y.S.; Zhang, M.; Fan, Y.B.; Boone, D.A. Quantitative comparison of plantar foot shapes under different weight-bearing conditions. *J. Rehabil. Res. Dev.* **2003**, *40*, 517–526. [[CrossRef](#)] [[PubMed](#)]
19. Tsung, B.Y.S.; Zhang, M.; Mak, A.F.T.; Wong, M.W.N. Effectiveness of insoles on plantar pressure redistribution. *JRRD* **2004**, *41*, 6A. [[CrossRef](#)]
20. Bousie, J.A.; Blanch, P.; McPoil, T.G.; Vicenzino, B. Contoured in-shoe foot orthoses increase mid-foot plantar contact area when compared with a flat insert during cycling. *J. Sci. Med. Sport* **2013**, *16*, 60–64. [[CrossRef](#)]
21. Losito, J.M. Impression casting techniques. In *Clinical Biomechanics of the Lower Extremity*; Valmassy, R., Ed.; Mosby: St. Louis, MO, USA, 1996.
22. Telfer, S.; Woodburn, J. The use of 3D surface scanning for the measurement and assessment of the human foot. *J. Foot Ankle Res.* **2010**, *3*, 19. [[CrossRef](#)]
23. Stanković, K.; Booth, B.G.; Danckaers, F.; Burg, F.; Vermaelen, P.; Duerinck, S.; Sijbers, J.; Huysmans, T. Three-dimensional quantitative analysis of healthy foot shape: A proof of concept study. *J. Foot Ankle Res.* **2018**, *11*, 8. [[CrossRef](#)] [[PubMed](#)]
24. Lee, Y.C.; Lin, G.; Wang, M.J. Comparing 3D foot scanning with conventional measurement methods. *J. Foot Ankle Res.* **2014**, *7*, 44. [[CrossRef](#)]
25. Cavanagh, P.R.; Rodgers, M. The Arch index: A useful measure from footprints. *J. Biomech.* **1987**, *20*, 547–551. [[CrossRef](#)]
26. Wagner Instruments. *Wagner FPTX Series Economy Manual Pain Threshold Testers; PAIN TEST™ ALGOMETER*: Greenwich, CT, USA; Available online: <http://www.wagnerinstruments.com/products/pain-test-algometer/fpk-fpn> (accessed on 1 February 2019).
27. Wibowo, D.B.; Haryadi, G.D.; Priambodo, A. Estimation of foot pressure from human footprint depths using 3D scanner. *AIP Conf. Proc.* **2016**, *1717*, 040008. [[CrossRef](#)]
28. Robinette, K.; Daanen, H. Precision of the CAESAR scan-extracted measurements. *ApplErgon* **2006**, *37*, 259–265. [[CrossRef](#)]
29. Wibowo, D.B.; Haryadi, G.D.; Widodo, A.; Rahayu, S.P. Estimation of calcaneal loading during standing from human footprint depths using 3D scanner. *AIP Conf. Proc.* **2017**, *1788*, 030063. [[CrossRef](#)]
30. Yung-Hui, L.; Wei-Hsein, H. Effects of shoe inserts and heel height on foot pressure, impact force, and perceived comfort during walking. *Appl. Ergon.* **2005**, *36*, 335–362. [[CrossRef](#)] [[PubMed](#)]
31. Druga, C.; Serban, I. Study of foot pressure-sole pressure sensor. In Proceedings of the 7th International Conference on Computational Mechanics and Virtual Engineering (COMEC) 2017, Brasov, Rumania, 16–17 November 2017.
32. Goske, S.; Erdemir, A.; Petre, M.; Budhabhatti, S. Reduction of plantar heel pressure: Insole design using finite element analysis. *J. Biomech.* **2006**, *39*, 2363–2370. [[CrossRef](#)] [[PubMed](#)]
33. Boehm, R. *The Foot & the Shoe: Measurement & Size*; DARCO (Europe) GmbH: Raisting, Germany, 2015.
34. Maiwald, C.; Grau, S.; Krauss, I.; Mauch, M.; Axmann, D.; Horstmann, T. Reproducibility of plantar pressure distribution data in barefoot running. *J. Appl. Biomech.* **2008**, *24*, 14–23. [[CrossRef](#)]
35. Cavanagh, P.R.; Rodgers, M.; Liboshi, A. Pressure distribution under symptom-free feet during barefoot standing. *Foot Ankle Int.* **1987**, *7*, 262. [[CrossRef](#)]
36. Shimizu, M.; Andrew, P.D. Effect of heel height on the foot in unilateral standing. *J. Phys. Ther. Sci.* **1999**, *11*, 95–100. [[CrossRef](#)]
37. Bonanno, D.R.; Landorf, K.B.; Menz, H.B. Pressure-relieving properties of various shoe inserts in older people with plantar heel pain. *Gait Posture* **2011**, *33*, 385–389. [[CrossRef](#)] [[PubMed](#)]

